Pergamon

0042-6989(95)00095-X

Vision Res. Vol. 36, No. 1, pp. 27–41, 1996

0042-6989/96 $9.50 + 0.00

The Binocular Computation of Visual Direction

J. STEPHEN MANSFIELD,*† GORDON E. LEGGE*

Received 18 August 1994; in revised form 21 March 1995

How is a single visual direction assigned to a binocular feature for which the left and right eyes are signaling different directions? According to geometrical principles, binocular visual direction is the average of the visual directions measured from the left and right eyes. Contrary to this prediction, we have found that the relative visual direction between two Gabor targets presented at different stereoscopic depths could be manipulated by varying the contrast ratio between the left and right images. This finding is consistent with a new model in which the relative alignment of depth features is determined from a maximum-likelihood combination of the direction signals from the left and right eyes. In a second experiment we provide support for this model, showing that the magnitude of the contrast-dependent bias in visual direction is predicted by the uncertainty for spatial localization in the left and right images. Lastly we show that visual direction and stereopsis have different dependencies on interocular contrast differences, suggesting that the computation of stereo depth and visual direction are mediated via different mechanisms.

Binocular vision Visual direction Stereopsis Contrast Ocular dominance

INTRODUCTION

To locate a feature in 3-dimensional space, both its depth and its visual direction need to be determined. Information concerning a feature's depth can be computed from the differences between the views from the left and right eyes, but, because a feature in depth projects to different locations on the left and right retinas, its visual direction is ambiguous. Nevertheless, provided the difference is not too large, the feature is usually seen in only one direction. How is a single visual direction assigned to a binocular feature for which the left and right eyes are signaling different directions?

The binocular computation of direction is of importance, not only to general theories of binocular space perception, but also to the stereoscopic perception of object shape. For example, Fig. 1A depicts the left and right eye's views that might be seen by someone hovering above a pyramid. The apex of the pyramid can be localized in depth using stereopsis. But to perceive the pyramid's correct shape, the visual direction of the apex relative to that of the base needs to be determined. If the left eye's view was used to infer the direction of the apex, then the pyramid would appear skewed to the right. If the right eye's view was used, then the pyramid would appear skewed to the left. In the fused percept neither of these views prevails—the apex of the pyramid is seen at a location midway between the left and right eye's views. The signals from the left and right eyes are combined to determine visual direction.

Absolute versus relative direction

The *absolute* visual direction of a target depends on two factors: (1) the oculocentric direction signals from the eyes (the local-signs from the left and right retinas); and (2) the directions in which the left and right eyes are pointing (see Ono, 1991 for a review). However, knowledge of absolute direction is not needed for visual tasks such as determining surface or object shape. To determine the shape of the pyramid in Fig. 1A it is only necessary to know the visual direction of the pyramid's apex relative to the direction of its base. The judgment of *relative* direction only requires oculocentric direction signals and is independent of the direction in which the eyes are pointing.

In our study we are concerned exclusively with how judgments of the relative direction between features in depth are determined by the binocular visual system.

A geometrical model

Figure 2 illustrates the geometry for calculating binocular visual direction. The left (L), and right (R), eyes are viewing point P while fixating at point F. The angles λ and ρ are the left and right oculocentric directions‡ of P with respect to F. Point B is the binoculus, the center for binocular visual direction. This is the location from which judgments of relative direction are made. It is commonly accepted that the binoculus is located on the vertical midline between the left and right eyes (Hering, 1879; Barbeito & Ono, 1979; see Ono, 1991 for a review).

*Department of Psychology, University of Minnesota, 75 East River Road, Minneapolis, MN 55455, U.S.A.
†To whom all correspondence should be addressed.
‡Oculocentric directions are measured from the nodal point of each eye.

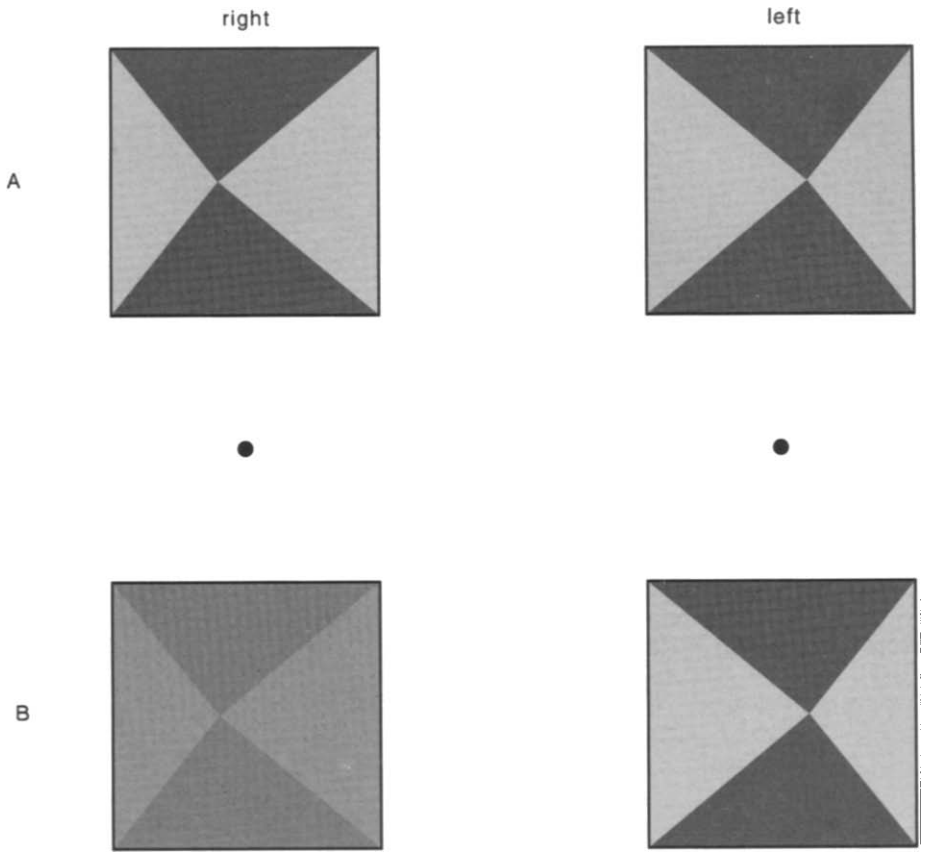

FIGURE 1. (A) Left and right eyes' views of a pyramid in depth (shown for crossed fusion). If the visual direction of the apex was determined from either of these views alone then the pyramid may be interpreted as being skewed in one direction or the other. However, in the fused percept the apex of the pyramid is located centrally. (B) Same view as above, except the right eye's image has reduced contrast. Even though the location of the apex in the left and right images has not been altered, the pyramid in the fused percept appears skewed to the right.

The angle β is the binocular visual direction of P with respect to F. Appendix A shows that β is closely approximated by the average of the left and right oculocentric directions:

$$\beta \approx \frac{\lambda + \rho}{2}. \quad (1)$$

This rule succinctly describes the subjective impression of the location of binocularly fused features (Wheatstone, 1838; Julesz, 1971; Ono, Angus & Gregor, 1977; Sheedy & Fry, 1979) and is consistent with a Keplerian projection theory for visual direction (see Ono, 1991).

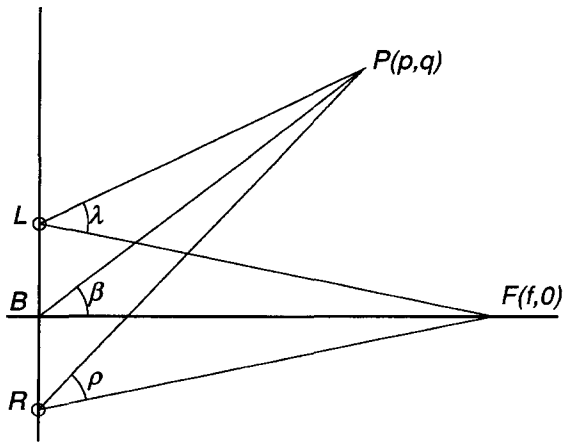

FIGURE 2. The geometry of binocular vision (see text for details).

Challenges to the geometrical model

Despite the appealing simplicity of the geometrical model, many studies have indicated that the combination of monocular signals in the calculation of binocular visual direction might not be so straightforward. If the left and right images of a line stereogram are given different luminance intensities, then the relative direction of the features in the stereogram is biased towards the view seen by the eye with the more intense image (Verhoeff, 1933; Fincham, in Charnwood, 1949). Figure 1B illustrates this phenomenon, showing the left and right images from Fig. 1A except the right eye's image has lower luminance contrast. In the fused percept, the pyramid appears skewed to the right. This effect also occurs in the binocular viewing of real 3-dimensional scenes—when one eye is covered with a neutral density filter, the perceived alignment of objects is biased towards the view seen by the unfiltered eye (Charnwood, 1949; Francis & Harwood, 1951). A similar direction bias can be induced using a +0.5 or +1.0 dioptres lens to blur the image in one eye (Charnwood, 1949), or simply by ocular dominance (Francis & Harwood, 1951;

Sheedy & Fry, 1979; Barbeito, 1981; Ono & Barbeito, 1982; Porac & Coren, 1986). These findings challenge purely geometrical models of binocular visual direction, suggesting instead that the left and right direction signals are weighted by parameters such as luminance, image resolution, and ocular dominance, at, or prior to, the stage of binocular combination.

Various mechanisms have been proposed to account for the changes in visual direction due to differences in image quality between the left and right eyes. Verhoeff (1935) explained his findings within a suppression theory of binocular direction, in which visual direction was that of the monocular view that received the most attention. Charnwood (1965) suggested that the effect was due to differential transmission times between cortical units within a neural representation of a Keplerian-type array. Dodwell (1970) and Sperling (1970) also proposed a modification to the connections between units within a Keplerian array that could produce changes in perceived visual direction under unequal monocular stimulation. Tyler (1983) has suggested that the visual direction of the binocularly-fused stimulus may be determined by integration over the direction responses of the component monocular inputs. While each of these explanations can qualitatively account for the visual direction of the binocularly-fused feature, none has achieved general acceptance, and the geometrical averaging rule is still widely accepted as a sufficient explanation for binocular visual direction (Ono & Mapp, 1995; although see Erkelens & van de Grind, 1994).

In our study we used a vernier alignment task to assess the influence of interocular contrast differences on the perceived direction between binocularly viewed Gabor targets. Similar to the effects of interocular differences in luminance or blur, our results show that binocular visual direction is biased towards the view seen by the eye with the higher contrast image. We have developed a new model for binocular direction which explains this finding. In our model, binocular visual direction is determined from a maximum-likelihood combination of the direction signals from the left and right eyes. The left and right signals are weighted by the directional uncertainty associated with their direction estimates. In a second experiment we provide quantitative support for our new model, showing that the magnitude of the contrast-dependent shift in visual direction is predicted by the uncertainties in the left and right monocular direction signals (estimated from the acuities for monocular vernier alignment). Lastly, we have compared the dependence of visual direction on interocular contrast differences with similar measures for stereoscopic depth perception. This comparison illustrates that the computation of stereo depth and visual direction may be mediated via different mechanisms.

EXPERIMENT 1: HOW CONTRAST AFFECTS VISUAL DIRECTION

Methods

Apparatus

Stereoscopic stimuli were displayed on two Apple high-resolution monochrome monitors with P4 (white) phosphor, maximum local-amplitude contrast 90%. The mean luminance of both displays was set to 48 cd/m^2. The two monitors were driven by separate graphics cards. For each card, the red, green and blue video signals were combined using the video-attenuator and software routines described by Pelli and Zhang (1991). These procedures enabled 12-bit gray-level resolution for each monitor.

The two screens were positioned side-by-side and were viewed from 1.72 m through a mirror stereoscope so that images presented on the left and right screens were viewed by the left and right eyes respectively. Prior to data collection, the optical apparatus was aligned with the displays so that the observer's vergence and direction of gaze were appropriate for viewing features centered on the midline 1.72 m in front of the observer. Differences in the pixel-array geometry between the two displays were smaller than one pixel over the area where the stimuli were displayed [assessed using a modification of the procedure described by Maloney and Koh (1988)].

Stimuli

The stimuli consisted of Gabor patches with luminance profile of the general form:

$$L(x, y) = \exp[-(x^2 + y^2)/(2s^2)]\cos(2\pi fx); \quad (2)$$

where x and y are the horizontal and vertical screen dimensions, s is the space constant for the Gaussian envelope which was set to 0.35 deg, and f is the carrier spatial frequency which was set to 1.0 c/deg.*

Two Gabor patches were displayed on each monitor so that the stereoscopically viewed percept was of two vertically-aligned Gabor targets (see Fig. 3). The location of each stereo-Gabor was determined by the following parameters:

- X: horizontal location, defined as $(L_x + R_x)/2$ (where L_x and R_x are the x coordinates for the center of the left and right Gabors),
- Z: binocular disparity, defined as $(L_x - R_x)$.

The vertical center-to-center spacing between upper and lower Gabors was 2.1 deg. A small, black, square fixation mark was positioned in the center of each screen between the upper and lower Gabors. Subjects were

*The mean luminance of cosine-phase Gabors marginally increases as contrast is increased. Such a luminance change potentially confounds our experimental findings as, when large enough, an interocular luminance difference can produce changes in visual direction (Charnwood, 1949; Francis & Harwood, 1951). This is unlikely in our study, though, because at the largest contrast ratios tested, the difference in the mean luminance of the Gabors was just 0.5%. Interpolation within the data from subject A2 in Francis and Harwood (1951) reveals that a 0.5% interocular luminance difference would be expected to produce a change in visual direction of only 5 sec arc. This is considerably smaller than the directional shifts measured here (see Results section) and is less than the vernier acuity measured with these stimuli (see Fig. 11).

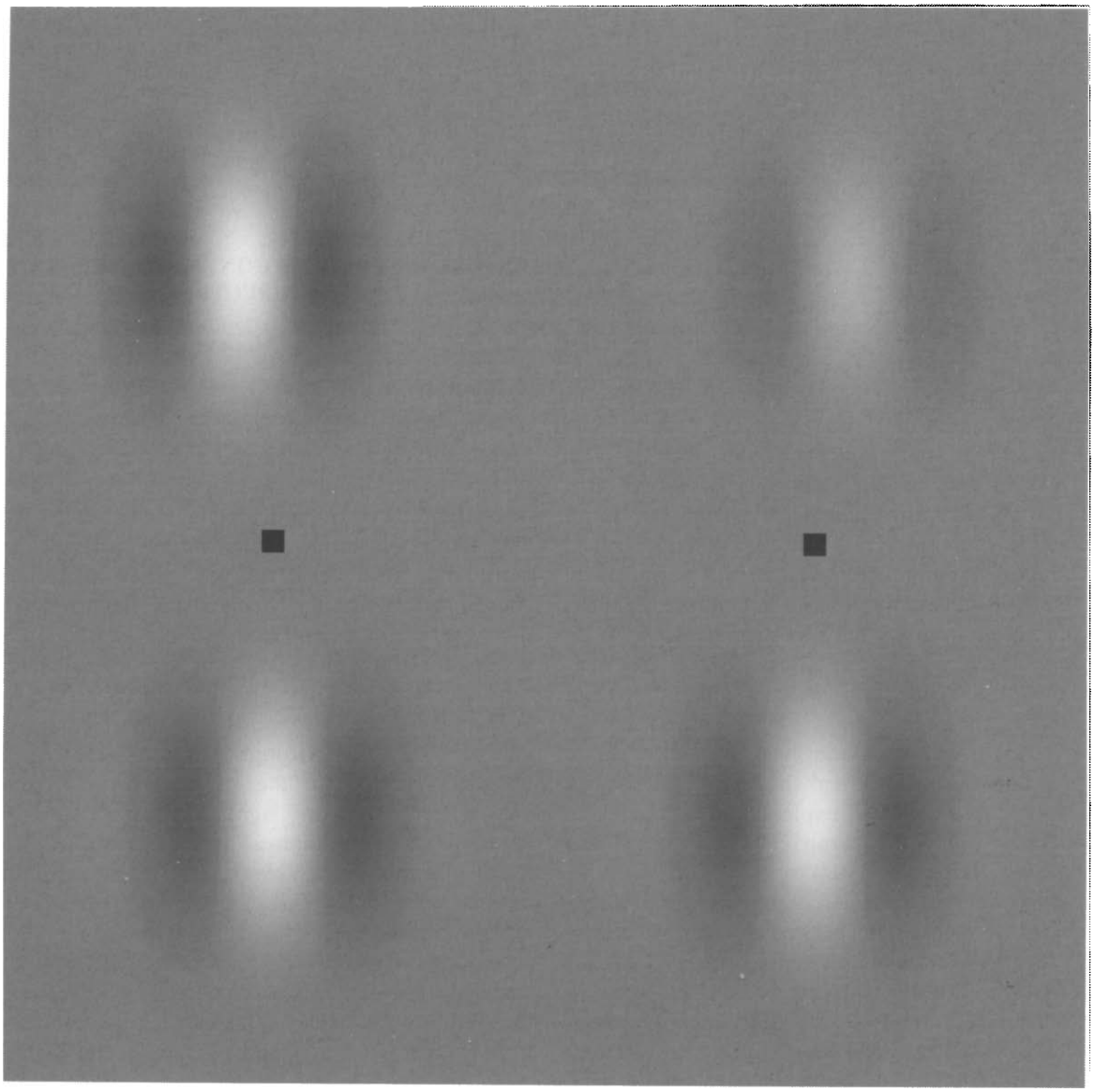

FIGURE 3. Example stereo-Gabors like those used in the experiments. With crossed fusion, the stereo percept is of two Gabor targets one vertically above the other. The upper Gabor has unequal contrast in the left and right eyes. The lower Gabor is on the fixation plane and the upper Gabor is in front of the fixation plane. The disparity was made by adding equal and opposite shifts to the horizontal locations of the upper Gabor's monocular images, so that according to the geometry of binocular vision, the two Gabors should appear vertically aligned. However, we find that the contrast difference between the left and right images shifts the perceived direction of the upper Gabor so that the targets appear misaligned. The direction of the misalignment is towards the direction of the monocular image with higher contrast.

instructed to maintain fixation on the fixation mark. Eye position ought not to influence the judgment of relative direction in these experiments, and it was not necessary to monitor eye fixation during the experiments.

Observers

Detailed measurements were collected from three observers, one of whom (JSM) was aware of the aims of the experiments. All observers had normal or corrected-to-normal vision, and all demonstrated the ability to perceive stereoscopic depth with the experimental stimuli.

Procedure

The stereo-Gabor in the top half of the screen was positioned on the vertical midline ($X = 0$ arc min) with a disparity (Z) of 30 arc min. The monocular contrasts of this Gabor were varied to give different interocular contrast ratios. The stereo-Gabor in the lower half of the screen always had equal contrast in the left and right images. A method-of-adjustment was used to modify the horizontal location (X) of the equal-contrast Gabor so that it appeared to be vertically aligned with the mixed-contrast Gabor. Alignment estimates were collected with the disparity (Z) of the equal-contrast Gabor set to 0, 15,

30, 45 and 60 arc min. These data could then be used to estimate the visual direction of the mixed-contrast target (see Results). The data reported here were collected only with crossed disparities. Preliminary observations indicated that the sign of the disparity, crossed or uncrossed, was not a critical parameter for our findings.*

The starting horizontal location of the equal-contrast Gabor was randomized for each adjustment procedure. Observers initiated each trial by pressing a key on the computer keyboard. The stereo stimulus was displayed for 1 sec, after which the observer indicated (by pressing either of two keys) whether the lower Gabor appeared to be misaligned to the left or right of the upper Gabor. On the following trial the X-location of the lower Gabor was shifted in the appropriate direction (as indicated by observer's response) to reduce the misalignment, by adding equal increments to L_x and R_x so that Z remained constant. The resolution for this adjustment was 0.25 pixels, corresponding to 10 sec arc. Sub-pixel accuracy was achieved by sub-sampling a high-resolution image of the Gabor stimulus. The procedure continued until the observer pressed a further key to indicate that the upper and lower Gabors appeared to be vertically aligned. The final X location of the lower Gabor was recorded.

One eye's image of the mixed-contrast Gabor was given a fixed contrast C, and the other eye's image was set to a lower contrast to achieve the required interocular contrast ratio. In the first series of alignment measurements, C was set to 25% (Michelson contrast) and the contrast ratios ranged from 1:1 to 1:5.7. In a second series of measurements, C was set to 50% and the contrast ratios ranged from 1:2 to 1:11.4. Each contrast ratio was tested with the left image having higher contrast than the right and with the right image having higher contrast than the left. Trials from two independent alignment procedures, in which the mixed-contrast target had the equal and opposite mixture of left and right contrasts, were randomly interleaved, so that it was impossible to predict which eye would receive the higher contrast image. Four alignment estimates were collected for each combination of contrast ratio and equal-contrast Gabor disparity.

Results

Figure 4 shows a subset of the data from the first experiment with $C = 25\%$ (some contrast-ratio conditions have been omitted for clarity). The plots show the X location at which the lower Gabor appeared to be vertically aligned with the upper Gabor (the point of perceived alignment—the PPA) as a function of the disparity (Z) of the lower Gabor. Each data point is the mean of the four alignment estimates. Lines connect data with the same mixed-contrast Gabor contrast ratio as indicated at the left of each plot.

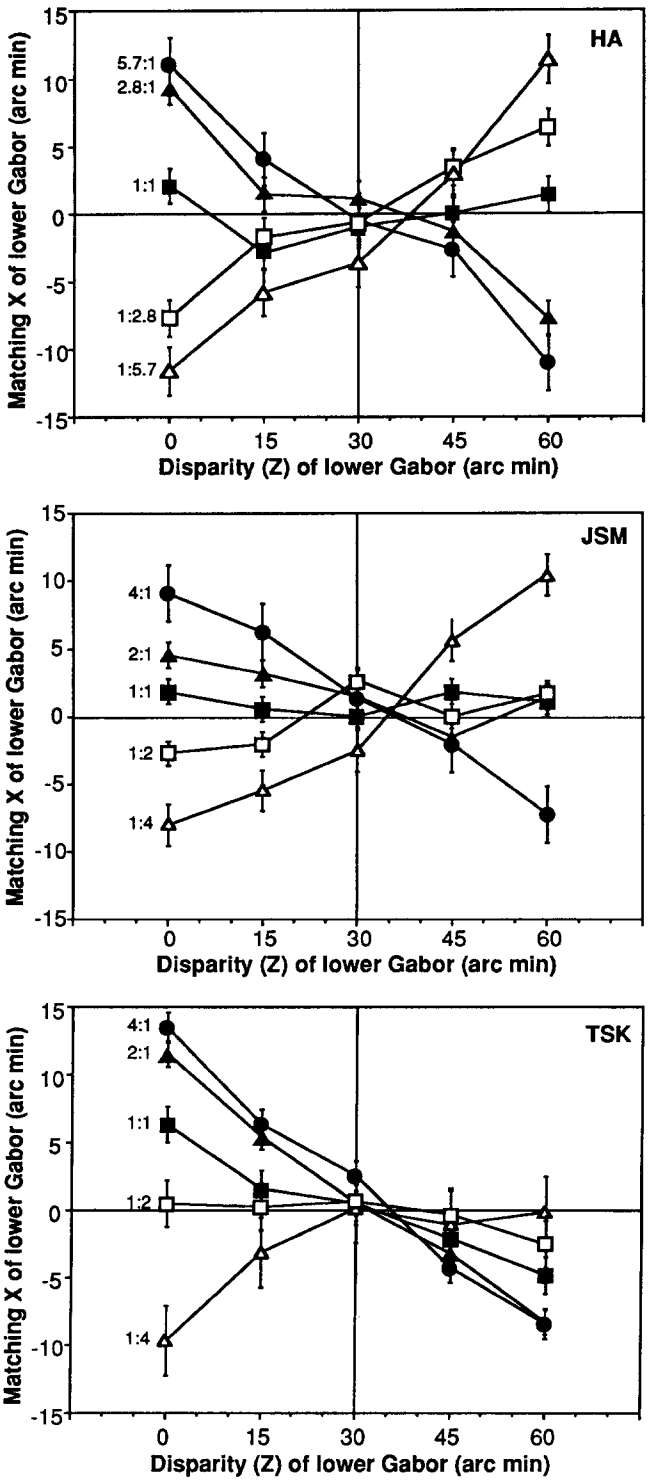

FIGURE 4. Data from the method of adjustment trials from three observers. The disparity of the mixed-contrast (upper) Gabor was 30 arc min. Each data point shows the X-location of the equal-contrast (lower) Gabor that appeared to be vertically aligned with the mixed-contrast Gabor. Data are shown for different L:R contrast ratios in the mixed-contrast (upper) Gabor as indicated at the left of each line. Contrast ratios were made with a fixed contrast C of 25%. Error bars indicate ± 1 SD for the alignment estimates.

If binocular visual direction was determined by the averaging model then all the PPAs would be expected to lie along the $X = 0$ horizontal line. For subjects HA and JSM this is only the case when the contrast ratio is 1:1.

*Mansfield and Legge (1995) report similar data collected with the mixed-contrast Gabor presented with either crossed or uncrossed disparity on randomly interleaved trials.

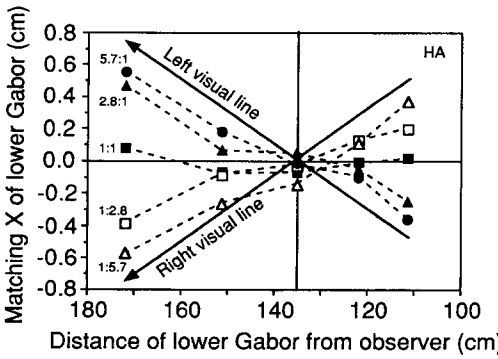

FIGURE 5. Data from observer HA in Fig. 4 replotted with X and Z transformed into physical distance. Solid lines represent the visual lines from the left and right eyes passing through the location of the upper Gabor. L:R contrast ratios are indicated at the left of each data set. Unequal contrast in the left and right eyes biases the points of perceived alignment towards the visual line of the monocular image with higher contrast.

Otherwise for all three observers it is clear that the PPA is dependent on both the contrast ratio of the upper Gabor and the disparity of the lower Gabor. For disparities greater than 30 arc min (i.e. in front of the upper Gabor), when the left eye has greater contrast than the right, the PPA is to the left of the point of true alignment, while for disparities less than 30 arc min (i.e. behind the upper Gabor), if the left eye has greater contrast than the right, then the PPA is to the right of the point of true alignment. The opposite is true when the right eye has the greater contrast. For the largest contrast ratios, the PPA is more than 10 arc min removed from the point of geometrical alignment.

While the data from subjects HA and JSM exhibit the same general trends, the data from TSK are somewhat different. The contrast ratio that gave performance closest to the geometrical prediction was 2:1, and when the lower Gabor was at a closer depth than the upper, the PPA was biased to the left irrespective of the contrast ratio.

A clearer picture of the data is given in Fig. 5 which replots one subject's data from Fig. 4. In this plot, disparity (Z) has been transformed to the physical distance in centimeters from the observer. Likewise X has also been converted into centimeters of displacement from the midline. Lines from the left and right eyes which pass through the location of the mixed-contrast Gabor are also plotted. This figure shows that the PPAs are shifted towards the visual line of the eye viewing the higher contrast image.

For each contrast ratio, the PPAs map out the line of points in depth which appeared aligned with the mixed-contrast Gabor (see Fig. 6). Given that these points were perceptually aligned they must share the same visual direction. The straight line fitted to these points can be thought of as the binocular visual line of the mixed-contrast Gabor. The orientation, B, of this line with respect to the veridical direction (straight ahead) indicates the change in visual direction of the mixed-contrast Gabor caused by the interocular contrast difference. For the purposes of describing the data, the angle B is taken as a measure of the binocular visual direction of the mixed contrast target. Figure 6 shows that the change in orientation of the binocular visual line is consistent with a corresponding change in the location of the binoculus. The binoculus is shifted towards the location of the eye receiving the higher contrast image. This change in location of the binoculus has been noted previously for interocular luminance differences (Charnwood, 1949; Francis & Harwood, 1951).

Figure 7 shows how B depends on interocular contrast ratio ($C = 25\%$). The alignment data for each contrast ratio were transformed into the same coordinates shown in Fig. 5. A least-squares method was used to find the best-fitting straight line to the data for each contrast ratio. The orientation of these lines (with respect to straight ahead) is plotted as a function of the contrast ratio of the mixed contrast Gabor. Straight ahead (the veridical direction of the mixed contrast target) has a binocular direction of zero. The left and right visual lines have directions (L and R as shown in Fig. 6) of -70 and $+70$ arc min respectively. For all observers it can be seen that the binocular visual line of the mixed contrast Gabor is biased towards the visual line of the eye seeing the higher contrast image. Figure 8 shows the data obtained with $C = 50\%$. These data are quite similar to those in Fig. 7, although the change in visual direction occurs more gradually as the contrast ratio is manipulated. The smooth curves plotted with these data are the best-fitting curves from our new model for binocular visual direction.

The bias exhibited by TSK in Fig. 4 is reflected in Figs 7 and 8 by a leftwards shift of his data-set. For this observer, a contrast ratio of 1:2.5 was required for veridical direction perception. This bias is consistent with a left ocular dominance in the determination of visual direction. Ocular dominance biases in measurements of visual direction have been reported previously

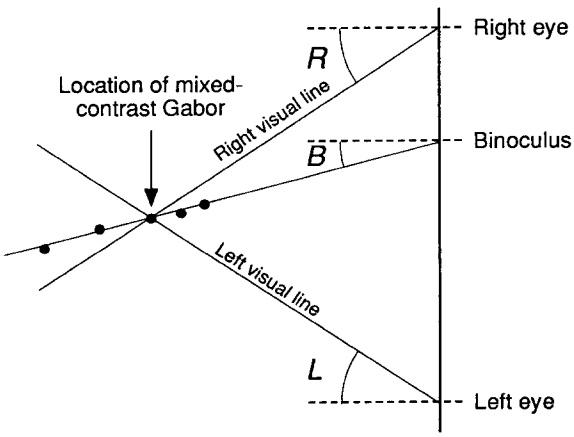

FIGURE 6. A straight line is fitted to the PPAs between the mixed-contrast Gabor and the equal-contrast Gabor. This is the binocular visual line for the mixed-contrast Gabor. The orientation of this line (B) compared to straight ahead is the change in visual direction caused by the unequal monocular contrasts. L and R indicate the orientation (with respect to straight-ahead) of the visual lines from the left and right eyes passing through the location of the mixed-contrast Gabor.

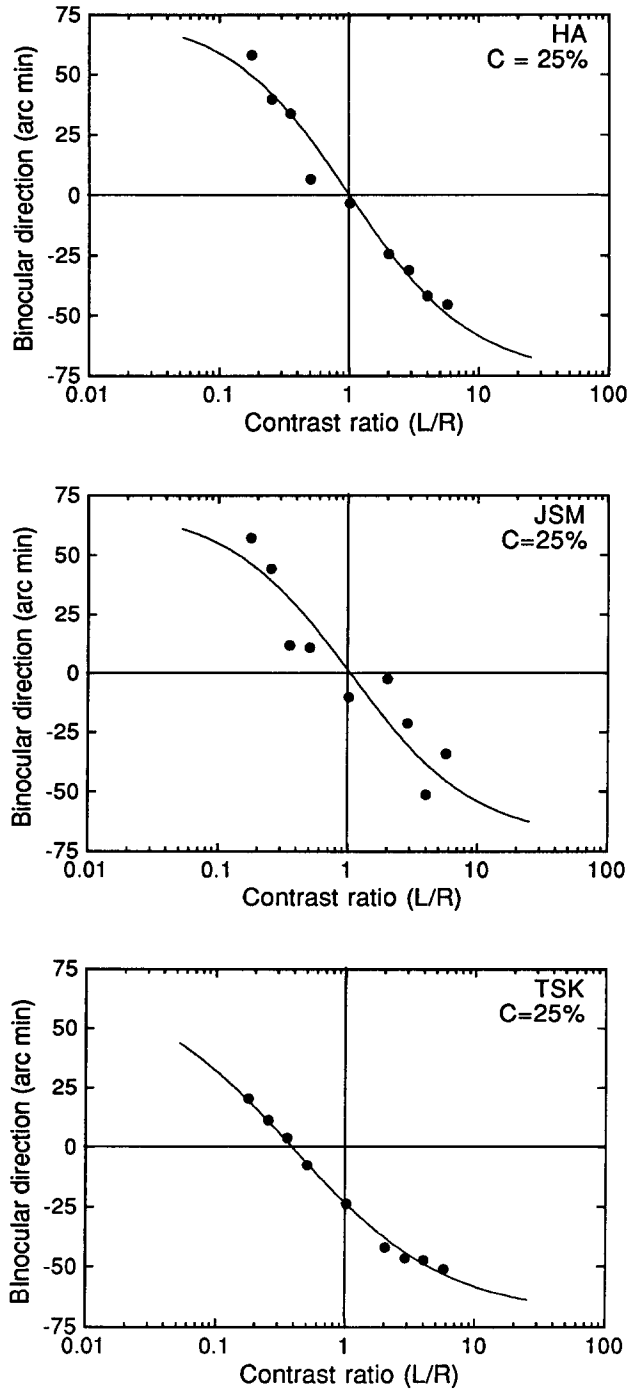

FIGURE 7. The dependence of visual direction (*B* in Fig. 6) on interocular contrast ratio. These graphs show data from the 3 observers for contrast ratios made with a fixed contrast, *C*, of 25%. Each data point is the arc-tangent of the slope of the best-fitting straight line to the alignment data for the given contrast ratio, and indicates the binocular direction of the mixed-contrast Gabor. A direction of zero corresponds to straight ahead, which was the veridical direction of the target. Directions of −70 and +70 arc min are the directions from the left and right eyes respectively. The smooth lines through the data are the best fitting curves from our new model (see text). The best fitting parameters are given in Table 1.

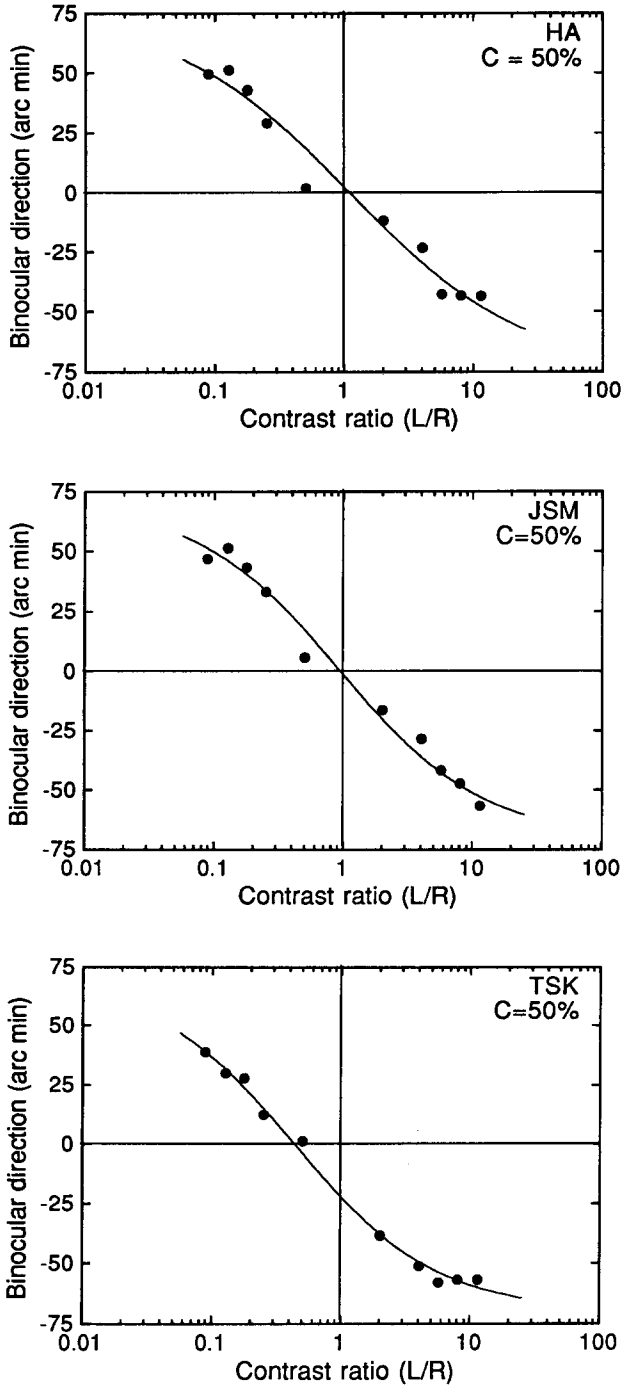

FIGURE 8. Same as Fig. 7, except $C = 50\%$.

(Francis & Harwood, 1951; Sheedy & Fry, 1979; Porac & Coren, 1986).

Discussion

The results from Experiment 1 indicate that the relative direction between binocular targets is dependent upon the strength of the contrast signal in the left and right eyes. Binocular visual direction is biased towards the direction of the visual line from the eye receiving the image with higher contrast. Thus, interocular contrast differences have a similar effect on visual direction as interocular differences in luminance (Verhoeff, 1933; Charnwood, 1949; Francis & Harwood, 1951) and blur (Charnwood, 1949).

Predictions from the geometrical model

How might the geometrical model predict the relative direction between the mixed-contrast and equal-contrast Gabors? Provided both targets are seen in stereoscopic

depth, their relative direction ought to be at the average of the direction differences signaled by the left and right eyes. However, if the left and right images of the mixed-contrast Gabor do not stereoscopically fuse, then the predictions from the geometrical model are less straightforward. For example, if the contrast in one eye is below detection threshold, the relative direction between the two Gabors will be governed by the eye that can still see both Gabors. Another possibility is that there may be a critical interocular contrast ratio above which stereo fusion is impossible (Smallman & McKee, 1995). If our mixed-contrast stimuli exceeded this limit, then they might be perceived as rivalrous or diplopic. The perceived alignment between the upper and lower Gabors will likely fluctuate between the views seen by either eye. [This was not a problem in our experiment, however, as none of the observers reported difficulty in fusing the stimuli, and the perceived depth of the mixed-contrast Gabor remained fairly constant for a wide range of contrast ratios (see Experiment 3).]

Even with a strict application of a contrast-ratio limit for fusion, our data do not support the geometric law. Figures 7 and 8 show that a 2:1 contrast ratio was sufficient to induce a noticeable change in visual direction. This ratio is within the fusion range measured by Smallman and McKee (1995), and the contrasts of the monocular images for this contrast ratio were both well above detection threshold.

A NEW MODEL FOR BINOCULAR VISUAL DIRECTION

In the geometrical model, the left and right oculocentric direction signals are combined directly to deduce binocular visual direction. This assumes that the left and right eyes can signal the oculocentric directions with arbitrary precision. However, it is likely that their signals will be affected by neural noise. The accuracy of each oculocentric direction signal will depend on the signal-to-noise ratio. Our new model uses *maximum-likelihood* principles to include the effect of noise in the binocular calculation of relative direction.

Rather than just signaling one value for the relative direction, the left and right eyes each provide a probability distribution for the difference in visual directions between the two targets. The peak of each *direction distribution* corresponds to the most-likely direction from that eye ($\hat{L}$ and $\hat{R}$), and the variance of the distribution corresponds to the uncertainty for that eye's estimate (σ_L^2 and σ_R^2). As the signal-to-noise ratio decreases, the directional uncertainty increases. In the model, the left and right direction signals are assumed to be independent estimates of visual direction. These signals are then combined to determine the most-likely direction in a manner similar to the *modified weak fusion* described by Maloney and Landy (1989). In Appendix B it is shown that the maximum-likelihood estimate for the binocular direction ($\hat{B}$) is given by the average of the monocular signals weighted by their associated uncertainties:

$$\hat{B} = \frac{\hat{L}/\sigma_L^2 + \hat{R}/\sigma_R^2}{1/\sigma_L^2 + 1/\sigma_R^2} = \frac{\hat{L}\sigma_R^2 + \hat{R}\sigma_L^2}{\sigma_L^2 + \sigma_R^2}. \quad (3)$$

Note that if σ_L^2 and σ_L^2 are equal then the above formula reduces to the simple geometrical model: $\hat{B} = (\hat{L} + \hat{R})/2$.

Modeling the effects of interocular contrast differences

We can relate our maximum-likelihood model to the psychophysical data collected in Experiment 1 by considering the effects of contrast on the accuracy of monocular visual direction judgments. Reducing the contrast of a feature increases the uncertainty with which it can be localized. Psychophysically, this relationship has been investigated using vernier acuity tasks. It is typically found that vernier acuity deteriorates as contrast is reduced (Watt & Morgan, 1983, 1984; Wilson, 1986; Bradley & Skottun, 1987; Klein, Casson & Carney, 1990; Banton & Levi, 1991; Krauskopf & Farrel, 1991; Hess & Holliday, 1992; Waugh & Levi, 1993; Whitaker, 1993). The change in vernier acuity, σ, with contrast is usually well described by an inverse power law: $\sigma \propto C^{-k}$, where C is contrast, and k is a parameter governing the slope of the contrast-versus-acuity function in log–log coordinates. This inverse power law can be incorporated in equation (3) to give:

$$\hat{B} = \frac{\hat{L}C_L^{2k} + \hat{R}C_R^{2k}}{C_L^{2k} + C_R^{2k}}, \quad (4)$$

where C_L and C_R are the contrasts of the left and right images.

The data from subject TSK in Experiment 1 suggest that there is an ocular dominance component in the calculation of visual direction. This can be included in the model as a further adjustment to the weights given to the signals from each eye so that:

$$\hat{B} = \frac{\hat{L}w_L C_L^{2k} + \hat{R}w_R C_R^{2k}}{w_L C_L^{2k} + w_R C_R^{2k}} \quad (5)$$

where w_L and w_R are the ocular dominance weights for the left and right eyes. Equation (5) can be re-written:

$$\hat{B} = \frac{WQ^{2k}\hat{L} + \hat{R}}{WQ^{2k} + 1}; \quad (6)$$

where $W = w_L/w_R$, and Q is the contrast ratio: $Q = C_L/C_R$.

Equation (6) relates binocular visual direction to the contrast ratio between the eyes. There are only two free parameters: k the exponent relating vernier acuity (and hence direction uncertainty) with stimulus contrast, and W, the ocular dominance, where $W > 1$ indicates a stronger weighting of the left eye's input, and $W < 1$ indicates a stronger weighting of the right eye's input. For most observers W would be expected to be 1.

The data in Figs 7 and 8 have been fitted with curves described by equation (6) using a maximum-likelihood curve fitting procedure with W and k free to vary. The best fitting parameters, along with the percentage of variance in the data accounted for by each curve fit, are

TABLE 1. Best-fitting parameters from the maximum-likelihood model for visual direction

	$C = 25\%$			$C = 50\%$		
Subject	k	W	%var	k	W	%var
HA	0.46	1.00	96.9	0.32	0.94	96.5
JSM	0.45	0.97	85.1	0.40	1.04	98.3
TSK	0.51	1.79	99.5	0.40	1.96	99.4

% var indicates the percentage of the variance in the visual direction data which is accounted for by the model.

shown in Table 1. For two observers W is very close to 1, while for the third W is closer to 2 reflecting a bias towards the left eye. The best fitting values for k are between 0.3 and 0.5. These k values are at the lower end of the range found in other psychophysical measurements of the change in vernier acuity with contrast. The model provides a close fit to the dependence of visual direction on interocular contrast ratio, accounting for 96% of the variance in the data.

EXPERIMENT 2: PREDICTING VISUAL DIRECTION WITH THE MAXIMUM-LIKELIHOOD MODEL

Our model relates the visual direction of a binocular depth target to the uncertainty for estimating the visual direction in the left and right eye's views. A critical parameter, as far as Experiment 1 is concerned, is the exponent k relating directional uncertainty to image contrast. The best fitting values for k seem to be lower than might be expected, thus it is not clear that changes in monocular direction uncertainty are sufficient to explain the change in perceived direction found in Experiment 1.

In this experiment we sought to provide quantitative support for our model. In one set of trials we measured monocular vernier acuity as a function of the contrast of the lower Gabor. Using the same stimulus configuration and image contrasts, we also measured the binocular visual direction of a mixed-contrast Gabor. Presumably, the monocular vernier acuity data would reflect the localization uncertainty for the monocular images in the binocular alignment trials. The monocular vernier acuities could then be used to derive an estimate for k, and this estimate can be used with equation (6) to predict the visual direction of the mixed-contrast Gabor.

Methods

Stimuli

The stimuli were similar to those used in Experiment 1. For the binocular alignment experiments, the upper stereo target had zero disparity and unequal contrast in the left and right eyes. The fixed contrast (C) was set at 64% and contrast ratios of 1:1, 1:2, 1:4, 1:8 and 1:16 were generated by presenting a reduced contrast Gabor to the other eye. The lower stereo target had equal contrast (64%) in each eye. Data were collected in interleaved blocks with the disparity of the equal-contrast target set to either 0 or 30 arc min. For the monocular acuity experiments the upper Gabor was given one of the 5 contrasts used in the binocular experiment. The contrast of the lower Gabor, however, was always set to 64%.

Subjects

Detailed data were collected from two observers. One was the author (JSM) and the other was naive of the aims of the experiment. Both observers had normal or corrected-to-normal vision, and each demonstrated the ability to perceive stereoscopic depth in the experimental display.

Procedure

Monocular and binocular vernier acuities were measured using a constant stimulus procedure. However, because in the binocular experiments the point of perceived alignment was initially unknown, each block of trials was preceded by a short adjustment procedure, similar to that used in Experiment 1. In this adjustment procedure, the initial X location of the lower Gabor was set randomly. After each presentation the observer pressed one of four keys to indicate whether the lower Gabor appeared to be misaligned to the left or the right of the upper Gabor (with four keys the observer could indicate that either a coarse or fine adjustment was required in either direction). On the subsequent trial the position of the lower Gabor was adjusted in the appropriate direction (either by 1 pixel or 0.25 pixels depending on the key struck by the observer) to reduce the perceived misalignment. Once the observer was satisfied that the upper and lower Gabors were aligned, the current X position of the lower Gabor was taken as the expected point of perceived alignment for the following constant-stimulus procedure. The alignment procedure was repeated for each test condition at the start of every block of trials.

In the constant-stimulus procedure, seven X locations were selected that spanned either side of the expected point of perceived alignment. On each trial, one of the seven locations was selected, and the observer was required to indicate whether the lower Gabor was misaligned to the left or the right of the upper Gabor. The presentation interval was 150 msec, short enough to rule out any explanations for the experimental effects based on changes in eye position. In each presentation an equal random shift was added to the horizontal locations of both the upper and lower Gabors. This shift did not affect the horizontal relation between the location of the upper and lower Gabors, but served to prevent the observers from making alignment judgments with respect to the fixation mark (which was always present in the center of the display). The observers' responses triggered the next trial. No feedback was given.

For trials measuring monocular vernier acuity, ten different conditions were randomly interleaved (measuring vernier acuity in the left and right eyes, with the contrast of the upper Gabor set to 0.64, 0.32, 0.16, 0.08 or 0.04). In trials measuring binocular perceived alignment, nine different conditions were randomly interleaved (measuring acuities with contrast ratios of 16:1,

8:1, 4:1, 2:1, 1:1, 1:2, 1:4, 1:8 or 1:16). In each block of trials, the seven X locations were each tested 10 times, and each block of trials was repeated 4 times, so that the resulting acuity and alignment estimates were based on 280 observations.

These data produced psychometric functions relating the probability of indicating that the lower Gabor appeared to the right of the upper Gabor, as function of the location of the lower Gabor. The psychometric functions were fitted with cumulative Gaussian curves, using the maximum-likelihood procedure outlined by Watson (1979), with the mean and standard deviation free to vary. The mean of these functions corresponds to the 50% point on the psychometric function, and hence the point where the upper and lower Gabor appeared aligned. The standard deviation of these functions, corresponding to the slope of the psychometric function, was taken as a measure of vernier acuity.

Results

Monocular vernier acuity deteriorated as contrast was reduced. These data were described well by an inverse power law: $\sigma \propto 1/C^k$. The coefficient, k, was estimated using linear regression of the data plotting log stimulus contrast versus log vernier acuity. Best fitting values of k were 0.27 for MRM and 0.17 for JSM. These values are lower than those estimated from Experiment 1, but this is consistent with the trend that higher fixed contrasts (C) produce smaller values for k (see Table 1).

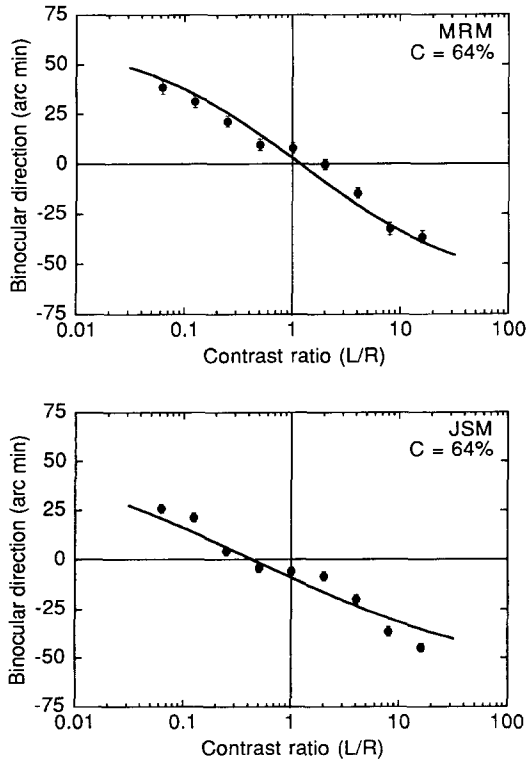

FIGURE 9. Prediction of visual direction using the maximum-likelihood model. These graphs show binocular direction as a function of interocular contrast ratio for two observers. Directions −63 and +63 arc min are the directions from the left and right eyes respectively. Error bars are the vernier acuities for making the alignment judgment and may be smaller than the data symbols. Contrast ratios were made with $C = 64\%$. The display duration was 150 msec. Smooth curves are the predicted visual directions according to equation (6) with k being determined from the monocular vernier acuity experiments. $k = 0.27$ (MRM), 0.17 (JSM).

Figure 9 shows the change in the direction of the binocular visual line caused by the interocular contrast differences. In this experiment, with the mixed-contrast Gabor at zero-disparity, the left and right monocular visual directions were −63 and +63 arc min respectively. Plotted with these data are the curves obtained by placing the appropriate values for k into equation (6). The curves from the model closely predict the actual change in visual direction, accounting for 97% (MRM) and 93% (JSM) of the variance in the data.

The outcome of this experiment supports the maximum-likelihood model for visual direction. The change in the binocular visual direction of the mixed contrast target can be predicted from the monocular vernier acuities.

The ocular dominance parameter W was free to vary in this analysis. The best fitting values were close to 1.0 for both observers. It may be possible to independently predict W from some other measure of ocular dominance. Coren and Kaplan (1973) grouped the many different ways to define and assess ocular dominance into three main classes: *sighting dominance* (a behavioral bias to use one eye for monocular tasks where either eye may be used), *sensory dominance* (a bias to see one eye's view during binocular rivalry), and *acuity dominance* (in which one eye performs more accurately on measures of acuity). Any of these factors might contribute to the left-eye directional dominance exhibited by observer TSK in our study. Perhaps the most likely measure would be ocular differences in monocular vernier acuity (Porac & Coren, 1986). Alternatively, it is quite possible that the dominance found in direction tasks like ours is unrelated to the other traditional measures of ocular dominance. As it was, all four subjects tested in Experiments 1 and 2 (including TSK) had a *right*-eye sighting preference and exhibited no ocular differences in monocular visual acuity, suggesting that these measures are unlikely to be major parameters if we were to account for ocular dominance in our model.

EXPERIMENT 3: COMPARISON WITH STEREO DEPTH PERCEPTION

What is the relationship between the perception of stereo depth and binocular visual direction? Under most normal circumstances the perception of stereoscopic depth is accompanied by binocular fusion. Even in circumstances where depth is perceived in the presence of diplopia, the perceived directions of the monocular images may be biased towards each other (Rose & Blake, 1988). Given that direction and depth need to be combined in order to perceive 3-dimensional scene layout, it is plausible that the same mechanism may mediate the computation of each. If this were the case, then stereo depth and visual direction might be expected to have a

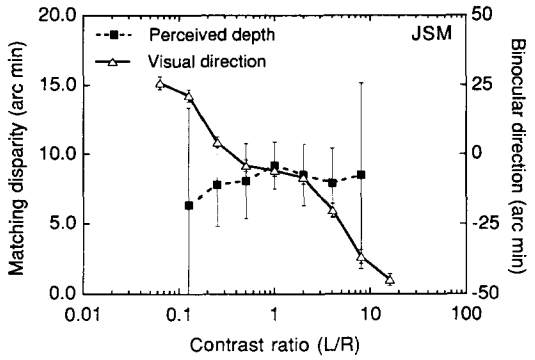

FIGURE 10. Comparing the effect of interocular contrast differences on binocular direction and perceived depth. Error bars indicate the vernier acuity or stereoacuity for performing the direction or depth matching task.

common dependence on interocular contrast differences. In this section we show that this is not so.

Methods

The stimulus configuration was similar to that used in Experiment 2. However, the upper Gabor was given a binocular disparity of 10 arc min, and the disparity of the lower Gabor was set to different values greater or less than 10 arc min in a constant stimulus procedure. The upper Gabor was given different interocular contrast ratios with a fixed contrast of 64% in one eye. The lower Gabor had equal contrast (64%) in both eyes. The subject's task was to indicate which of the stereo Gabors appeared furthest in front of the fixation plane. These data produced psychometric functions relating the disparity of the equal contrast Gabor to the proportion of trials on which it was seen with greater depth than the mixed contrast Gabor. These data were fitted with cumulative Gaussian curves. The disparity corresponding to the 50% point was taken as the perceived depth of the mixed contrast Gabor. The standard deviation of the cumulative Gaussian (corresponding to the slope of the psychometric function) was taken as an estimate of stereo acuity.

Results

These data were collected with the same set of contrast ratios used in Experiment 2, so we can compare any changes in stereo-depth perception with the corresponding changes in binocular visual direction.

Figure 10 compares changes in perceived depth and perceived direction as a function of the interocular contrast ratio. The visual direction data are replotted from Fig. 9. The same contrast ratios that produce large changes in visual direction only lead to slight and inconsistent changes in perceived depth.

These results are in accord with previous studies. Blake and Cormack (1979) reported that the magnitude of the tilt in depth, produced by dichoptic viewing of vertically oriented gratings of slightly different spatial frequencies, is not affected by interocular contrast ratios as large as 10:1. More recently, Rohaly and Wilson (1993) have shown that the perceived depth of a Gabor patch is unaffected by introducing a contrast difference between the eyes. Neurophysiological recordings from disparity-sensitive units in cat visual cortex reveal that the magnitude of the disparity-dependent response remained constant when the contrast of one eye's input was reduced by a factor of 10 (Freeman & Ohzawa, 1990).

Figure 11 compares changes in stereoacuity and binocular vernier acuity as a function of interocular contrast ratio. The binocular vernier acuity data were obtained from the slopes of the psychometric functions measured in Experiment 2, and show that changes in binocular vernier acuity are only slight as contrast ratio is changed. However, stereoacuity deteriorates rapidly as the interocular contrast ratio is changed from 1:1.

The stereoacuity data are in agreement with previous studies (Halpern & Blake, 1988; Legge & Gu, 1989). The small changes in binocular vernier acuity found here are predicted by the maximum-likelihood model (see Appendix B). Binocular vernier acuity should be best when the left and right eyes have equal contrast, but should slightly deteriorate as the contrast in one eye is reduced. Less weight is given to monocular signals with high uncertainty, so binocular vernier acuity should never be poorer than the acuity of the most sensitive eye. When the stimulus in one eye is below detection threshold, binocular vernier acuity will be equivalent to the monocular acuity of the other eye. Such a pattern of results has been reported for the effects of interocular-contrast-ratio differences on visual acuity (Cagenello, Arditi & Halpern, 1993).*

GENERAL DISCUSSION

Comparison with the computation of stereo depth

The results from this study indicate that the perception of stereo depth and binocular visual direction have

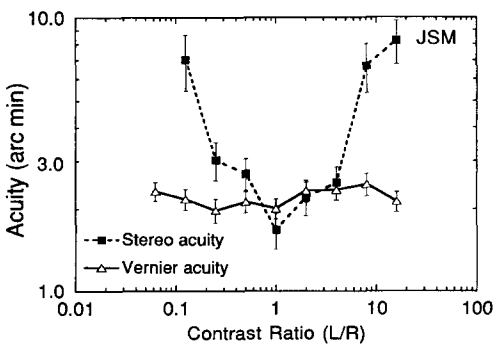

FIGURE 11. Comparing the effect of interocular contrast differences on binocular vernier acuity and stereoacuity. Error bars show standard deviations.

*It should be noted that our maximum-likelihood model predicts a $\sqrt{2}$ binocular enhancement of acuity (see Appendix B). In general, measurements of binocular summation for acuity tasks are somewhat lower than this prediction (Frisen & Lindblom, 1988; Cagenello *et al.*, 1993) except for hyperacuity tasks with small separations between the hyperacuity stimuli (Lindblom & Westheimer, 1989; Banton & Levi, 1991).

very different dependencies on interocular contrast differences. Stereoacuity rapidly deteriorates as interocular contrast differences are introduced (Halpern & Blake, 1988; Legge & Gu, 1989), whereas any detriment in binocular vernier acuity is significantly less marked. Conversely, perceived depth is unaffected by interocular contrast differences (Blake & Cormack, 1979; Rohaly & Wilson, 1993), while visual direction is markedly distorted. These comparisons underline a fundamental difference between the perception of stereo depth and binocular direction: stereo depth perception requires that the stimulus is detected in both eyes (Hawken, Parker & Simmons, 1987; Simmons, 1992; Simmons & Kingdom, 1994), whereas visual direction can be determined with a detectable stimulus in either or both eyes. Thus the accuracy for stereo depth judgments is limited by the noise in the least sensitive monocular channel (Legge & Gu, 1989) while the accuracy for binocular direction judgments is limited by the noise in the most sensitive monocular channel. This argument suggests that, even though the integration of direction and depth information is required for perception of 3-dimensional spatial layout, the actual computation of direction and depth are quite different processes. This conclusion is consistent with results from Ono *et al.* (1977) who noted that, with brief presentation durations and low luminance, binocular fusion was possible without the fused target appearing at the depth predicted by its disparity.

What might be the nature of the neural mechanisms that signal binocular visual direction? Ohzawa, De Angelis and Freeman (1990) have proposed a neural architecture that underlies neurons ideally suited as disparity detectors. An important quality of their disparity neuron is that the disparity response is independent of the visual direction of the stimulus (provided it is within the binocular receptive field). This property is brought about through a specific combination of monocular simple cells in quadrature phase whose squared responses are summed at the site of binocular combination according to: $C = (\cos L + \cos R)^2 + (\sin L + \sin R)^2$, where C is the response of the binocular complex cell, $\sin L$ and $\cos L$ are the responses from left monocular simple cells with sine and cosine phase, and $\sin R$ and $\cos R$ are the right monocular simple cells. A similar architecture can be used to construct hypothetical neurons with responses that are tuned to the *visual direction* of the binocular stimulus independent of binocular disparity. Such neurons are obtained if the right-eye's sine response is subtracted from that of the left rather than being added. This differencing operation can be realized by inverting the phase of the sine component of the right receptive field. This scheme suggests a more general organization of simple-cell connections than that proposed by Ohzawa *et al.* (1990), with connections between simple-cell units which feed into an array of complex cells, some of which would respond to binocular disparity, others to binocular direction. Multiple units of this type would probably be needed to implement the maximum-likelihood model.

A new law for visual direction

The geometry of binocular vision predicts that the visual direction of the binocularly fused stimulus should be midway between the visual directions seen by the left and right eyes. We have presented data which clearly indicate that, when calculating the relative direction of features in depth, the perceived direction is biased towards the direction signaled by the eye receiving the image with higher contrast. This outcome complements the earlier finding that interocular differences in luminance or blur influence the perceived spatial layout of features in depth (Verhoeff, 1933; Charnwood, 1949, 1965; Francis & Harwood, 1951). We have described a new model (equation 3) which explains the changes in visual direction introduced by interocular differences in contrast in terms of choosing the most likely direction given the noisy direction estimates signaled by the left and right eyes. Presumably this model could be applied to the experimental conditions tested by Verhoeff (1933), Charnwood (1949) and Francis and Harwood (1951).

While the maximum-likelihood model may be superficially similar to the geometrical averaging rule, it is important to note that it is founded on a totally different basis. The maximum-likelihood model is related to the modified-weak-fusion approach used by Maloney and Landy (1989) to model the contribution of different depth cues in determining a single perceived depth (see also Young, Landy & Maloney, 1993). Landy (1993) has used a similar scheme to account for the perceived location of a texture edge defined by conflicting texture cues.

Erkelens and van de Grind (1994) measured the point of perceived alignment (PPA) between a monocularly and a binocularly viewed target. They found that the PPA was determined exclusively by the eye seeing both targets. Their stimulus corresponds to an untested case in our contrast ratio experiment: where the mixed-contrast Gabor has zero contrast in one eye. For such stimuli, the alignment judgment cannot be performed by the eye that sees just one target, so that according to our model, that eye's direction signal will have infinite uncertainty and will make no contribution to the computation of the direction difference between the targets. Thus, the situation investigated by Erkelens and van de Grind (1994) is at one extreme of a continuum of different levels of interocular combination in the determination of visual direction. An important characteristic of our model is that it can account for visual direction with either binocular or monocular viewing conditions.

One practical consequence of our findings is that patients with a monocular cataract or who have a monovision refractive correction* will likely misperceive the precise spatial layout of objects in depth. It remains to be seen whether this effect persists over prolonged exposure to unequal ocular input, and if so, whether this distortion of binocular space presents a substantial functional deficit.

*In preference to a bi-focal prescription, different optical corrections are sometimes prescribed for the left and right eyes so that one eye is used for distant vision and the other for near vision.

REFERENCES

Banton, T. & Levi, D. L. (1991). Binocular summation in vernier acuity. *Journal of the Optical Society of America, A8*, 673–680.

Barbeito, R. (1981). Sighting dominance: an explanation based on the processing of visual direction in tests of sighting dominance. *Vision Research, 21*, 855–860.

Barbeito, R. & Ono, H. (1979). Four methods of locating the egocenter: a comparison of their predictive validities and reliabilities. *Behaviour Research Methods and Instrumentation, 11*, 31–36.

Blake, R. & Cormack, R. H. (1979). Does contrast disparity alone generate stereopsis? *Vision Research, 19*, 913–915.

Bradley, A. & Skottun, B. C. (1987). Effects of contrast and spatial frequency on vernier acuity. *Vision Research, 27*, 1817–1824.

Cagenello, R., Arditi, A. & Halpern, D. L. (1993). Binocular enhancement of visual acuity. *Journal of the Optical Society of America, A10*, 1841–1848.

Charnwood, J. R. B. (1949). Observations on ocular dominance. *The Optician, 116*, 85–88.

Charnwood, J. R. B. (1965). *Essay on binocular vision.* New York: Haffner.

Coren, S. & Kaplan, C. P. (1973) Patterns of ocular dominance. *American Journal of Optometry and Archives of the American Academy of Optometry, 50*, 282–292.

Dodwell, P. C. (1970). *Visual pattern recognition.* New York: Holt, Rinehart & Winston.

Erkelens, C. J. & van de Grind, W. A. (1994). Binocular visual direction. *Vision Research, 34*, 2963–2969.

Francis, J. L. & Harwood, K. A. (1951). The variation of the projection center with differential stimulus and its relation to ocular dominance. In *Transactions of the International Congress* (pp. 75–87). London: British Optical Association.

Freeman, R. D. & Ohzawa, I. (1990). On the neurophysiological organization of binocular vision. *Vision Research, 30*, 1661–1676.

Frisen, L. & Lindblom, B. (1988). Binocular summation in humans: evidence for a hierarchic model. *Journal of Physiology, London, 402*, 773–782.

Halpern, D. L. & Blake, R. (1988). How contrast effects stereoacuity. *Perception, 17*, 483–495.

Hawken, M. J., Parker, A. J. & Simmons, D. R. (1987). Human thresholds for a stereoscopic depth-discrimination task are no higher than those for simple monocular detection. *Journal of Physiology, London, 396*, 137P.

Hering, E. (1879). *Spatial sense and movements of the eye* (trans. Radde, C. A. 1942). Baltimore: American Academy of Optometry.

Hess, R. F. & Holliday, I. E. (1992). The coding of spatial position by the human visual system: effects of spatial scale and contrast. *Vision Research, 32*, 1085–1097.

Julesz, B. (1971). *Foundations of cyclopean perception.* Chicago, Ill.: University of Chicago Press.

Klein, S. A., Casson, E. & Carney, T. (1990). Vernier acuity as dipole and line detection. *Vision Research, 30*, 1703–1719.

Krauskopf, J. & Farrel, B. (1991). Vernier acuity: Effects of chromatic content, blur and contrast. *Vision Research, 31*, 735–749.

Landy, M. S. (1993). Combining multiple cues for texture edge localization. In Rogowitz, B. E. and Allebach, J. P. (Eds) *Human vision, visual processing, and digital display IV.* Proceedings of the SPIE, 1913.

Legge, G. E. & Gu, Y. (1989). Stereopsis and contrast. *Vision Research, 29*, 989–1004.

Lindblom, B. & Westheimer, G. (1989). Binocular summation of hyperacuity tasks. *Journal of the Optical Society of America, A6*, 585–589.

Maloney, L. T. & Koh, K. (1988). A method for calibrating the spatial coordinates of a visual display to high accuracy. *Behavior Research, Methods, Instruments, and Computers, 20*, 373–389.

Maloney, L. T. & Landy, M. S. (1989). A statistical framework for robust fusion of depth information. *Visual Communications and Image Processing IV. Proceedings of the SPIE, 1199*, 1154–1163.

Mansfield, J. S. & Legge, G. E. (1995). Is there more than one cyclopean eye for visual direction? *Investigative Ophthalmology and Visual Science, 36*, S813.

Marr, D. & Poggio, T. (1979). A computational theory of human stereo vision. *Proceedings of the Royal Society of London B, 204*, 301–328.

Mayhew, J. E. W. & Frisby, J. P. (1981). Psychophysical and computational studies towards a theory of human stereopsis. *Artificial Intelligence, 17*, 349–385.

Ohzawa, I., De Angelis, G. C. & Freeman, R. D. (1990). Stereoscopic depth discrimination in the visual cortex: neurons ideally suited as disparity detectors. *Science, 249*, 1037–1041.

Ono, H. (1991). Binocular visual directions of an object when seen as single or double. In Regan, D. (Ed.) *Vision and visual dysfunction*, Vol. 9, *Binocular vision.* (pp. 1–18). London: Macmillan.

Ono, H. & Barbeito, R. (1982). The cyclopean eye vs the sighting dominant eye as the center of visual direction. *Perception & Psychophysics, 32*, 201–210.

Ono, H. & Mapp, A. P. (1995). A restatement and modification of Wells-Hering's laws of visual direction. *Perception, 24*, 237–252.

Ono, H., Angus, R. & Gregor, P. (1977). Binocular single vision achieved through fusion and suppression. *Perception & Psychophysics, 21*, 513–521.

Pelli, D. G. & Zhang, L. (1991). Accurate control of contrast on microcomputer displays. *Vision Research, 31*, 1337–1350.

Porac, C. & Coren, S. (1986). Sighting dominance and egocentric localization. *Vision Research, 26* 1709–1713.

Rohaly, A. M. & Wilson, H. R. (1993). The role of contrast in depth perception. *Investigative Ophthalmology and Visual Science, 34(Suppl.)*, 1437.

Rose, D. & Blake, R. (1988). Mislocalization of diplopic images. *Journal of the Optical Society of America A, 2*, 1512–1521.

Sheedy, J. E. & Fry, G. A. (1979). The perceived direction of the binocular image. *Vision Research, 19*, 201–211.

Simmons, D. R. (1992). Spatiotemporal properties of stereoscopic mechanisms. D. Phil thesis, University of Oxford, England.

Simmons, D. R. & Kingdom, F. A. A. (1994). Contrast thresholds for stereoscopic depth identification with isoluminant and isochromatic stimuli. *Vision Research, 34*, 2971–2982.

Smallman, H. S. & McKee, S. P. (1995). A contrast ratio constraint on stereo matching. *Proceedings of the Royal Society of London, Series B, 260*, 265–271.

Sperling, G. (1970). Binocular vision: a physical and neural theory. *American Journal of Psychology, 83*, 461–534.

Tyler, C. W. (1983). Sensory processing of binocular disparity. In Schor, C. M. & Ciuffreda, K. J. (Eds) *Vergence eye movements: basic and clinical aspects.* Boston, Mass.: Butterworth.

Verhoeff, F. H. (1933). Effect on stereopsis produced by disparate retinal images of different luminosities. *Archives of Ophthalmology, 10*, 640–644.

Verhoeff, F. H. (1935). A new theory of binocular vision. *Archives of Ophthalmology, 13*, 152–175.

Watson, A. B. (1979). Probability summation over time. *Vision Research, 19*, 515–522.

Watt, R. J. & Morgan, M. J. (1983). The recognition and representation of edge blur: evidence for spatial primitives in spatial vision. *Vision Research, 23*, 1465–1477.

Watt, R. J. & Morgan, M. J. (1984). Spatial filters and the localization of luminance change in human vision. *Vision Research, 24*, 1387–1397.

Watt, R. J. & Morgan, M. J. (1985). A theory of the primitive spatial code in human vision. *Vision Research, 25*, 1661–1674.

Waugh, S. J. & Levi, D. M. (1993). Visibility, timing and vernier acuity. *Vision Research, 33*, 505–526.

Wheatstone, C. (1838). Contributions to the physiology of vision—Part the first. On some remarkable and hitherto unobserved, phenomena of binocular vision. *Philosophical Transactions of the Royal Society, 128*, 371–394.

Whitaker, D. (1993). What part of a vernier stimulus determines performance? *Vision Research, 33*, 27–32.

Wilson, H. R. (1986). Responses of spatial mechanisms can explain hyperacuity. *Vision Research, 26*, 453–469.

Young, M. J., Landy, M. S. & Maloney, L. T. (1993). A perturbation analysis of depth perception from combinations of texture and motion cues. *Vision Research, 33*, 2685–2696.

Acknowledgements—This research was supported by NIH grant EY02857 and AFOSR 90-0274. Preliminary reports of these data have been given at the annual meeting of the Association for Research in Vision and Ophthalmology, Sarasota, Fla., 1992 and 1993.

APPENDIX A

Geometry of Visual Direction

Figure 2 shows the left and right eyes viewing point $P(p, q)$ while fixating at $F(f, 0)$. Angles λ, ρ, and β are the visual direction of P with respect to F as viewed by the left (L) and right (R) eyes and the binoculus (B) respectively. If the interocular separation is $2i$, then:

$$\tan\lambda = \frac{f(q-i)+pi}{fp-i(q-i)} \tag{A1}$$

$$\tan\rho = \frac{f(q+i)-pi}{fp+i(q+i)} \tag{A2}$$

$$\tan\beta = \frac{q}{p}. \tag{A3}$$

Double angle formulas show that:

$$\tan(\lambda+\rho) = \frac{2pq}{p^2-q^2+i^2} \tag{A4}$$

$$\tan(2\beta) = \frac{2pq}{p^2-q^2}. \tag{A5}$$

Thus if i^2 is small compared to (p^2-q^2) then:

$$\beta \approx \frac{\lambda+\rho}{2} \tag{A6}$$

the binocular visual direction from a binoculus located midway between the left and right eyes is approximated by the average of the left and right visual directions.

Figure A1 illustrates the regions of binocular visual space where equation (A6) provides a poor approximation. This plot assumes fixation on the vertical midline, but is otherwise independent of viewing distance. Solid curves in the upper plot are contours where $(\lambda+\rho)/2 = \alpha$, for $\alpha = 10, 20, 30, 40, \ldots, 80$ deg. The corresponding dashed lines show the binocular visual direction. The horizontal and vertical axes show distance in cm. For large viewing distances the curves asymptote to the dashed lines. The difference between the averaging model and the true visual direction is shown as a contour plot in the lower part of the figure. Here the contours map out $(\lambda+\rho)/2-\beta = \delta$ for $\delta = 0.5, 1, 2, 4, \ldots, 32$ arc min. The regions where the approximation is poor are located either side of the midline close to the observer. Most studies of stereopsis or visual direction use stimuli situated far removed from the areas where the averaging model is a poor approximation.

APPENDIX B

The Maximum-Likelihood Model for Binocular Visual Direction

(i) Binocular visual direction

According to most current models of spatial localization, stimuli are first filtered through linear bandpass spatial frequency channels and the resultant neural wave form is processed to extract specific spatial primitives such as zero-crossings (Marr & Poggio, 1979), peaks or troughs (Mayhew & Frisby, 1981) or centroids (Watt & Morgan, 1985). In the absence of neural noise these features can be localized with arbitrary precision, but if the neural wave form is noisy the accuracy for localization will be dependent on the signal-to-noise ratio (Legge & Gu, 1989). In the noisy wave form, localization estimates will cluster around the correct location. The mean accuracy of localization depends on the distribution of the localization estimates. If the distribution is broad the accuracy will be low. Legge and Gu (1989) show that the location distribution for zero-crossings is approximately Gaussian.

In our model for binocular visual direction we relate the location distribution in each eye to a Gaussian probability-density function. For example, from the left eye's neural image, $P_L(\theta)$, the probability of the target direction being θ is given by:

$$P_L(\theta) = \frac{\exp[-(\theta-\hat{L})^2/(2\sigma_L^2)]}{\sigma_L\sqrt{2\pi}} \tag{B1}$$

where $\hat{L}$ and σ_L are the mean and standard deviation of the left eyes direction distribution.

In our model, the left and right eye's direction distributions are combined to determine the *most-likely* visual direction. From Bayes theorem, if the left and right eyes provide independent estimates of visual direction then:

$$P(B\,|\,L, R) = \frac{P(L, R\,|\,B)P(L)P(R)}{P(B)} \tag{B2}$$

where $P(L)$ and $P(R)$ are visual-direction probability distributions. $P(L, R\,|\,B)$ and $P(B)$ are the prior probabilities for the binocular visual direction which, for this analysis, will be assumed constant. Equation (B2) can be re-written as

$$P(B\,|\,L, R) \propto P(L)P(R) \tag{B3}$$

so that

$$\max[P_B(\theta)] = \max\left[\frac{\exp-\{(\theta-\hat{L})^2/(2\sigma_L^2)+(\theta-\hat{R})^2/(2\sigma_R^2)\}}{2\pi\sigma_L\sigma_R}\right]. \tag{B4}$$

By differentiation it can be shown that the maximum value for the expression in equation (B4) is given when

$$\frac{(\theta-\hat{L})}{\sigma_L^2} + \frac{\theta-\hat{R}}{\sigma_R^2} = 0. \tag{B5}$$

Thus the most-likely visual direction is given by

$$\hat{B} = \frac{\hat{L}\sigma_R^2 + \hat{R}\sigma_L^2}{\sigma_L^2+\sigma_R^2}. \tag{B6}$$

It can be seen that this is the mean of the left and right direction signals weighted by their respective directional uncertainties:

$$\hat{B} = \frac{\hat{L}/\sigma_L^2 + \hat{R}/\sigma_R^2}{1/\sigma_L^2 + 1/\sigma_R^2}. \tag{B7}$$

(ii) Binocular vernier acuity

Binocular vernier acuity corresponds to the directional uncertainty associated with the binocular direction signal σ_B. σ_B^2 can be expressed in terms of the σ_L^2 and σ_R^2 as follows:

$$\sigma_B^2 = \sigma_L^2\left(\frac{\partial B}{\partial L}\right)^2 + \sigma_R^2\left(\frac{\partial B}{\partial R}\right)^2 + 2\sigma_{LR}^2\left(\frac{\partial B}{\partial L}\right)\left(\frac{\partial B}{\partial R}\right). \tag{B8}$$

In our model the left and right signals are assumed to be independent, so the covariance term σ_{LR}^2 can be set to zero. Substituting the appropriate values into equation (B8):

$$\sigma_B^2 = \sigma_L^2\left(\frac{\sigma_R^2}{\sigma_L^2+\sigma_R^2}\right)^2 + \sigma_R^2\left(\frac{\sigma_L^2}{\sigma_L^2+\sigma_R^2}\right)^2 \tag{B9}$$

$$= \frac{\sigma_L^2\sigma_R^2}{\sigma_L^2+\sigma_R^2}. \tag{B10}$$

This equation predicts the directional uncertainty for binocular visual direction from the uncertainties for the direction signals from the left and right eyes.

Rearranging equation (B10) it can be shown that binocular vernier acuity should never be poorer than the best monocular acuity. The model predicts quadratic summation for binocular acuity:

$$\frac{1}{\sigma_B} = \sqrt{\frac{1}{\sigma_L^2}+\frac{1}{\sigma_R^2}}. \tag{B11}$$

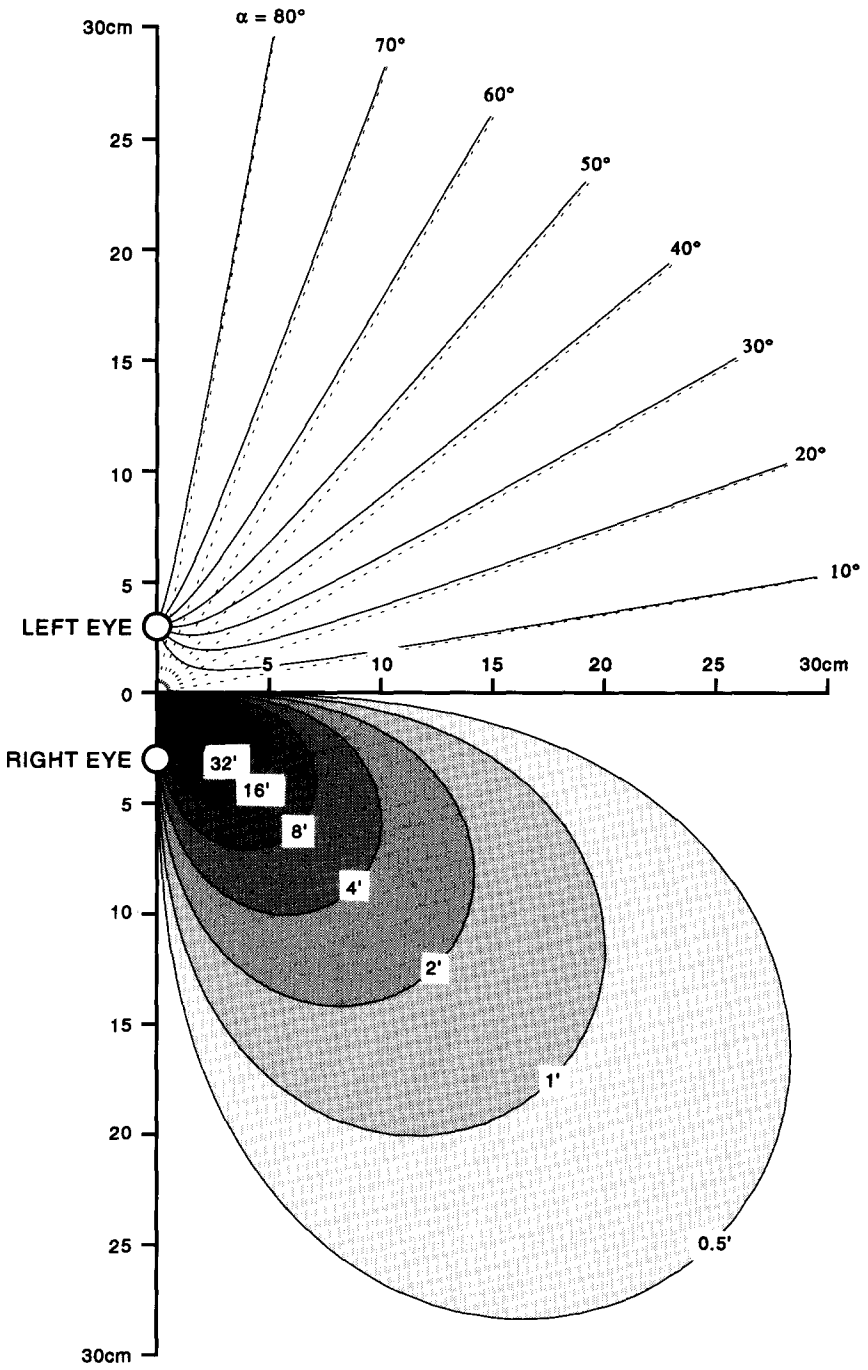

FIGURE A1. Comparison of the averaging model for visual direction and the veridical visual direction. This figure shows visual space in the horizontal plane through the eyes. Circles on the vertical axis indicate the location of the left and right eyes. Axes labels show the distance from the origin. The curves in the upper part of the figure plot contours of equal-visual direction. Solid curves are given by $(\lambda + \rho)/2 = \alpha$ (the Hillebrand hyperbolae), dashed lines are given by $\beta = \alpha$, where λ and ρ are the left and right oculocentric visual directions, and β is the veridical binocular visual direction between a central fixation point $(f, 0)$ and another point (p, q) as shown in Fig. 2. Values for α are shown around the circumference. The lower part of the figure shows the difference between the averaging model and the veridical direction in the form of a contour plot. Each contour is given by $(\lambda + \rho)/2 - \beta = \delta$. Values for δ are shown on each contour.